Electronic Supplementary Information

Chemicals and materials

Sodium tetrachloropalladate (Na_2PdCl_4), indium chloride ($InCl_3$), L-ascorbic acid (AA), *N*,*N*-dimethylformamide (DMF), polyvinylpyrrolidone (PVP, MW=40000), Nafion 117 solution (5 wt%) and indium oxide (In_2O_3) were supplied by Aladdin. Ethylenediamine (EN) was provided from Sinopharm Chemical Reagent Co. Ltd. (Shanghai, China). Molybdenum hexacarbonyl ($Mo(CO)_6$) was purchased from Macklin. All chemicals were used as received without any further purification.

Synthesis of the Mo-PdIn BNRs

For a typical synthesis of Mo-PdIn BNRs, AA (80 mg), $Mo(CO)_6$ (50 mg) and PVP (600 mg, MW=40000) were added to 2 mL of EN in a glass via to dissolve ultrasonically. Subsequently, 0.1 mL $InCl_3$ (0.1 M DMF solution) and 0.3 mL Na_2PdCl_4 (0.1 M DMF solution) were added to the above solution and sonicated to mix evenly. Then putting it into the 120 °C oil bath for 8 h. Finally, after mixture cooled to room temperature, the Mo-PdIn BNRs are collected by alternate centrifugation (10000 rpm) washing with acetone, ethanol, and deionized water. For comparison, Mo-PdIn-50 BNRs and Mo-PdIn-200 BNRs samples were synthesized by the same method except adding different amounts of $InCl_3$ precursors (50μl, 200μl), respectively.

Synthesis of the Mo-Pd MNRs

As a control sample, the synthesis method is the same as the above Mo-PdIn BNRs synthesis except that $InCl_3$ is not added.

Synthesis of the PdIn BNRs

As a control sample, the synthesis method is the same as the above Mo-PdIn BNRs synthesis except

that the addition of $Mo(CO)_6$ is replaced by the introduction of carbon monoxide.

General characterization

A ZEISS Gemini 500 scanning electron microscope (SEM) configured with energy-dispersive X-ray spectroscopy (EDX) was used to characterize the morphology and elemental distribution of the catalyst. Finer structural information of the catalyst was obtained by transmission electron microscopy (TEM) with a JEM-2100F. The crystal structure of the catalyst was obtained by a DX-2700 X-ray diffractometer (XRD). The elemental composition and electronic states of the catalysts were measured with an X-ray photoelectron spectroscopy (XPS) model ULVAC PHI Quantera. The ultraviolet–visible (UV–Vis) absorption was obtained by a TU-1900 spectrophotometer. The gas products were analyzed by a gas chromatograph (GC-2014 Shimadzu). The element components of the sample were measured via the inductively coupled plasma optical emission spectroscopy (ICP-OES, Agilent7700). The liquid products were analyzed by an Avance III HD 500 (Bruker) employed to collect nuclear magnetic resonance (NMR) spectroscopy.

Electrochemical measurements

All electrochemical measurements were performed on a CHI 760E electrochemical workstation. Electrocatalytic performance of urea synthesis was measured by a H-type three-electrode cell. Ag/AgCl electrode served as reference electrodes and a carbon rod as the counter electrode. The electrocatalyst ink was prepared via adding 4 mg of electrocatalyst to a 1 mL mixture containing 980 μL of ethanol and 20 μL of Nafion 117 (5 wt%). The preparation of the working electrode was described as follows, the Mo-PdIn BNRs or Mo-Pd MNRs electrocatalyst ink was sprayed on a 1×1 cm^2 hydrophobicity carbon paper with a loading of 0.4 mg cm^{-2} and dried naturally. During electrochemical measurements, high-purity CO_2 was continuously bubbled into a 0.1 M KNO_3

solution at the cathode at a constant flow rate of 20 sccm. All potentials were finally normalized to RHE reference scale (E (*vs.* RHE) = E (*vs.* Ag/AgCl) + 0.197 + 0.059 × pH).

Product quantification

The diacetylmonoxime method was typically applied to detect urea if the NO_2^- concentration is lower than 20 ppm.[1] Solution A, comprising 100 mL concentrated phosphoric acid, 300 mL concentrated sulfuric acid and 100 mg ferric chloride dissolved in 600 mL deionized water. Solution B, 0.5 g diacetylmonoxime, 10 mg aminothiourea and 100 mL deionized water. Then 2 mL of solution A and 1 mL of solution B was added into 1 mL of electrolyte solution after diluting. After heating at 110 ℃ for 15 min and cooling, the absorbance of the solution at 525 nm was measured by UV-Vis spectroscopy. The concentration of urea was calculated according to the calibration of the standard urea solution concentration-absorbance curve.

The possible NO_3^- reduction products (NH_3, NO_2^-) were quantified using the spectrophotometric method based on the calibration curves. Specifically, ammonia content was measured using the indophenol blue method[2]: 2.0 mL of 1 M sodium hydroxide aqueous solution containing 5% sodium citrate and 5% salicylic acid, 1.0 mL of 0.05 M sodium hypochlorite solution, and 0.2 mL of 1% mass fraction of sodium nitroxycyanide aqueous solution were added in sequence. In 2.0 mL of diluted electrolyte, mix the above solution evenly, place it in a dark environment to react for 2 h, and finally measure the absorbance at 665 nm. The amount of ammonia was computed according to the calibration of the standard ammonia concentration-absorbance curve. The concentration of NO_2^- was quantified by the Griess method.[2] Specifically, 0.4 g sulfonamide, 0.02 g naphthylethylenediamine hydrochloride and 1 mL phosphoric acid were dissolved in 5 mL water as a color developer, and 5 mL of diluted electrolyte was mixed with 0.1 mL of chromogenic reagent, and after 20 min of color

development, color development was performed with a UV-visible spectrophotometer, and the absorbance was recorded at 540 nm. The amount of nitrite was calculated according to the calibration of the standard nitrite concentration-absorbance curve.

The quantitative analysis of H_2 and CO was conducted by GC with a thermal conductivity detector and flame ionization detectors.

Product yield rate and Faradaic efficiency (FE) were calculated using the equations:

Urea yield rete = $C_{urea} \times V/ (m \times t)$

$FE_{urea} = 16 \times F \times C_{urea} \times V/ (60.06 \times Q)$

$FE_{NH_3} = 8 \times F \times C_{NH_3} \times V/ (17 \times Q)$

$FE_{NO_2^-} = 2 \times F \times C_{NO_2^-} \times V/ (46 \times Q)$

$FE_{CO} = 2 \times F \times n_{CO}/ Q$

$FE_{H_2} = 2 \times F \times n_{H_2}/ Q$

Where C_{urea} is urea concentration, V is catholyte volume, m is the catalyst weight (mg) , t is reaction time, F is Faraday constant (96485 C mol^{-1}), C_{NH_3} refers to the concentration of ammonia, $C_{NO_2^-}$ refers to the concentration of nitrite, Q is the total amount of charges passing the electrode.

In-situ Fourier transform infrared (FTIR):

The Experiments were performed in a NicoletiS50 spectrometer equipped with a liquid nitrogen-cooled MCT detector. The working electrode was prepared by spreading the configured catalyst suspension evenly over the surface of a gold-plated semi-cylindrical silicon prism. Pt electrode and Ag/AgCl electrode were used as the counter and reference electrodes. The 0.1 M KNO3 solution served as the electrolyte with CO_2-saturated. Each spectrum was obtained with a time resolution of 32 seconds, and the background spectrum of the electrode is obtained at the open circuit voltage

before the test. The voltage with measured potential range is -0.2~-0.6 V *vs.* RHE.

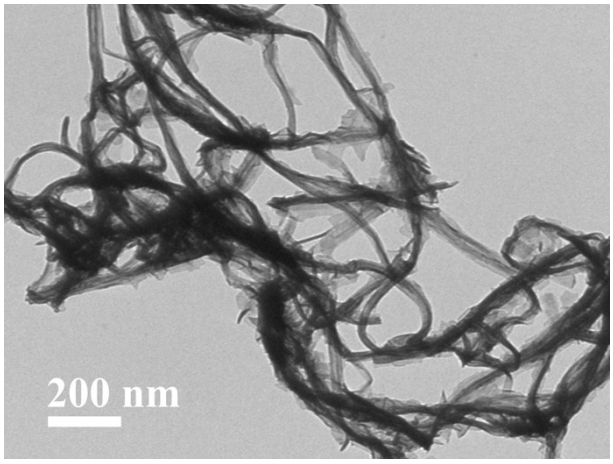

Fig. S1 TEM image of the Mo-Pd MNRs.

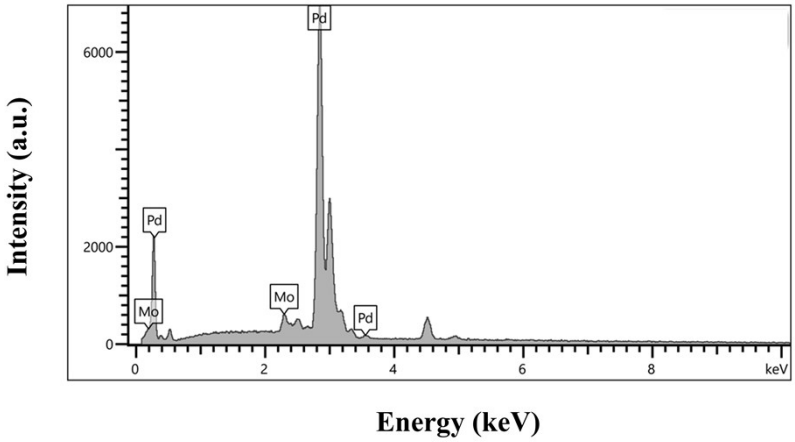

Fig. S2 EDX spectrum of the Mo-Pd MNRs.

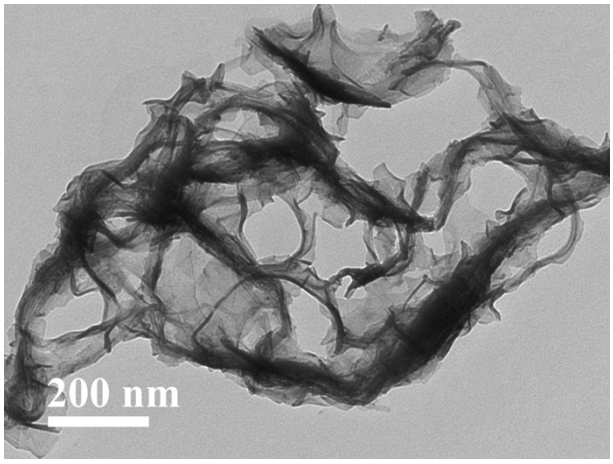

Fig. S3 TEM image of the PdIn BNRs.

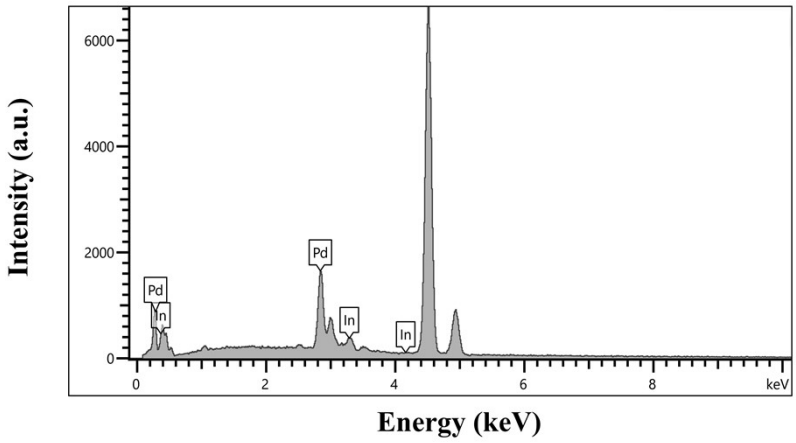

Fig. S4 EDX spectrum of the PdIn BNRs.

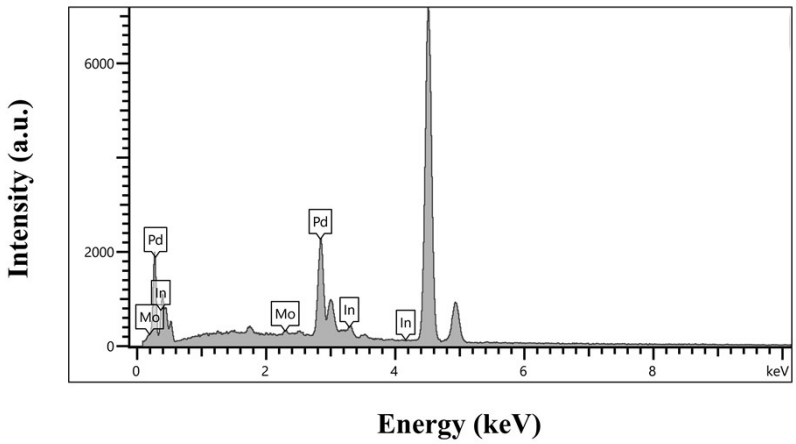

Fig. S5 EDX spectrum of the typical Mo-PdIn BNRs.

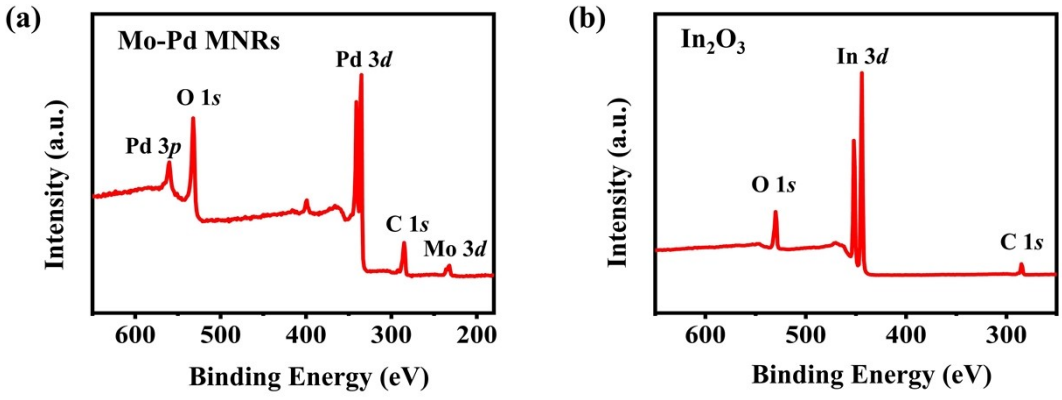

Fig. S6 XPS survey spectra of the (a) Mo-Pd MNRs and (b) commercial In_2O_3.

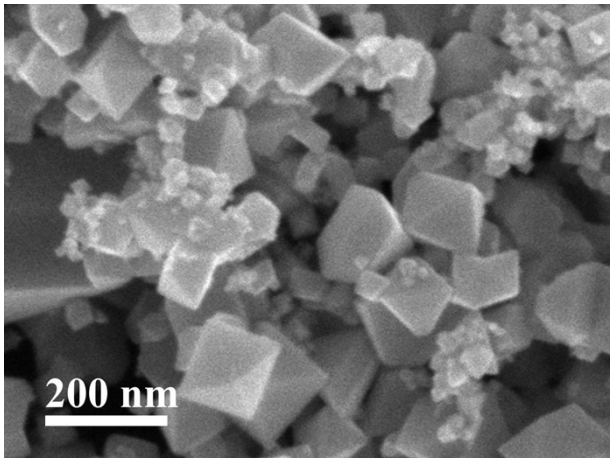

Fig. S7 SEM image of In_2O_3.

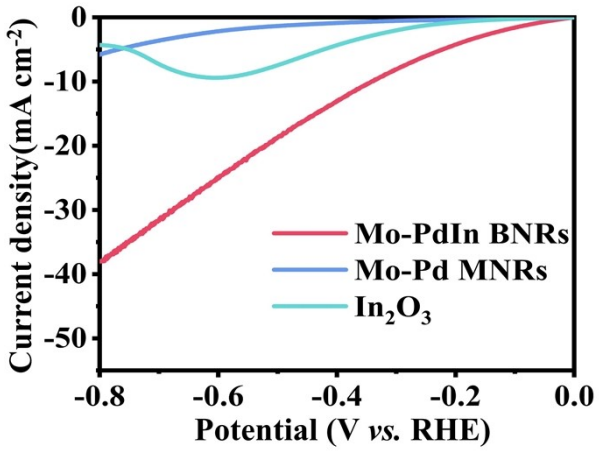

Fig. S8 LSV curves of Mo-PdIn BNRs, Mo-Pd MNRs and In_2O_3 in 0.1 M KNO_3 solution with flowing CO_2.

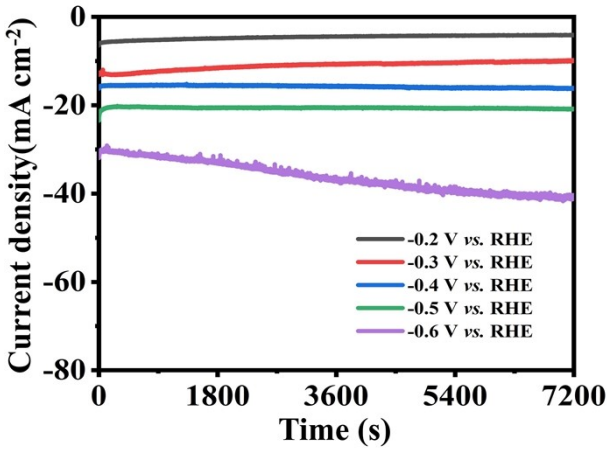

Fig. S9 Chronoamperometric curves of the Mo-PdIn BNRs for co-reduction of CO_2 and NO_3^- under different potentials.

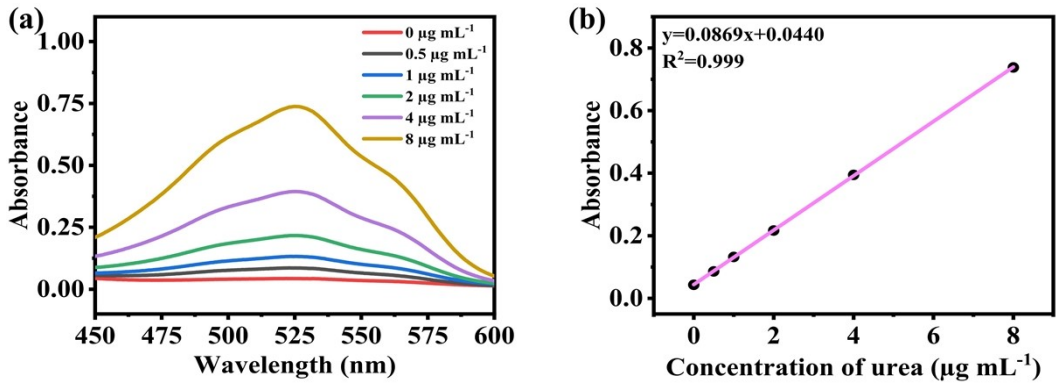

Fig. S10 (a) UV-Vis spectra of standard urea solution with various concentrations. (b) The corresponding calibration curve.

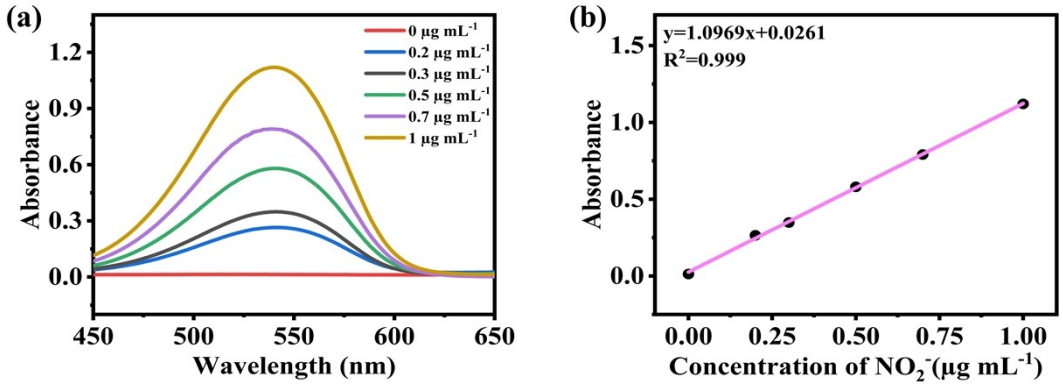

Fig. S11 (a) UV-Vis spectra of standard NO_2^- solution with various concentrations. (b) The corresponding calibration curve.

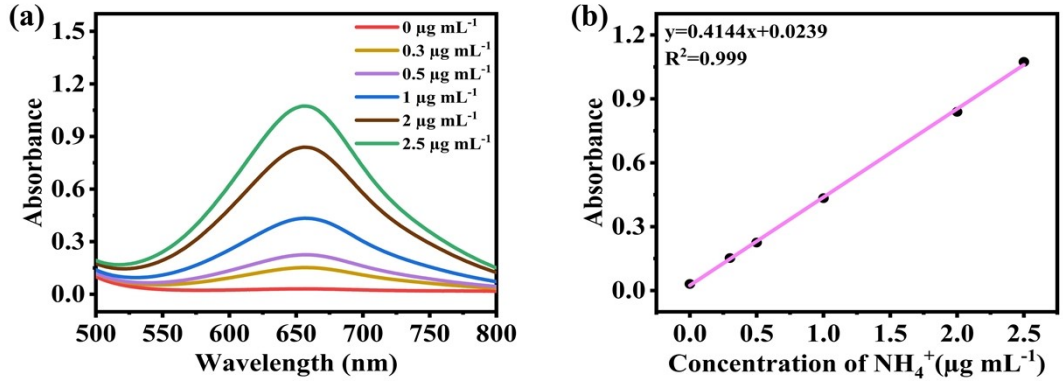

Fig. S12 (a) UV-Vis spectra of standard NH_4^+ solution with various concentrations. (b) The corresponding calibration curve.

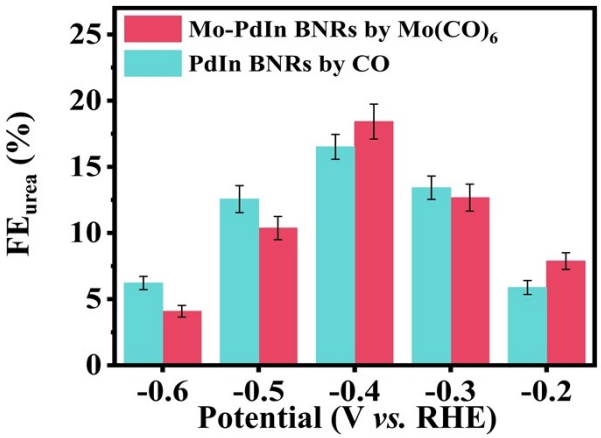

Fig. S13 The FE of urea with Mo-PdIn BNRs or PdIn BNRs at different applied potentials.

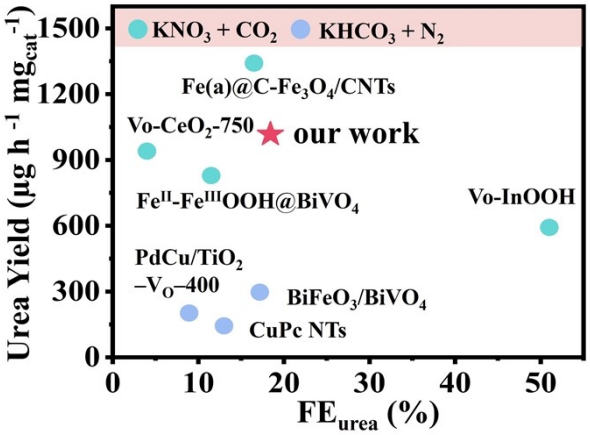

Fig. S14 Comparison of urea FE and yield rate of Mo-PdIn BNRs with some other reported catalysts.

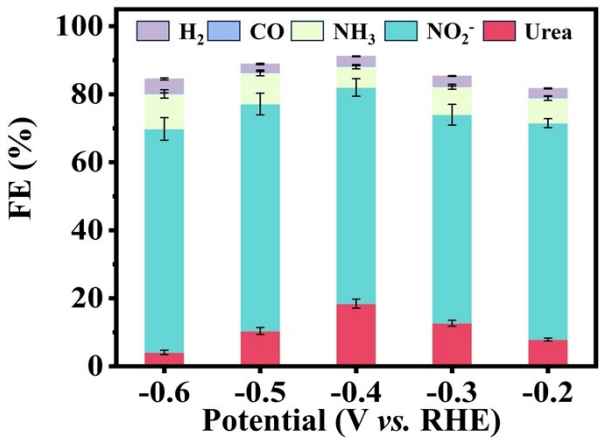

Fig. S15 FEs of main products of CO_2 and NO_3^- co-reduction on the Mo-PdIn BNRs.

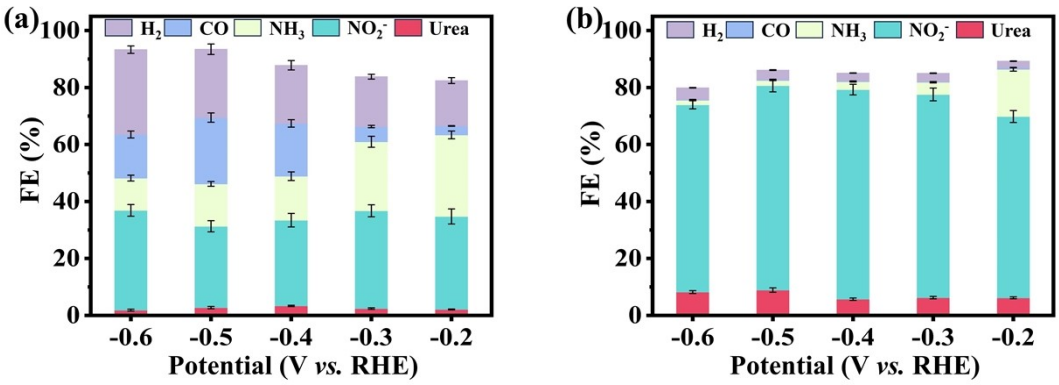

Fig. S16 (a) FEs of main products of CO_2 and NO_3^- co-reduction on the Mo-Pd MNRs. (b) FEs of main products of CO_2 and NO_3^- co-reduction on the In_2O_3.

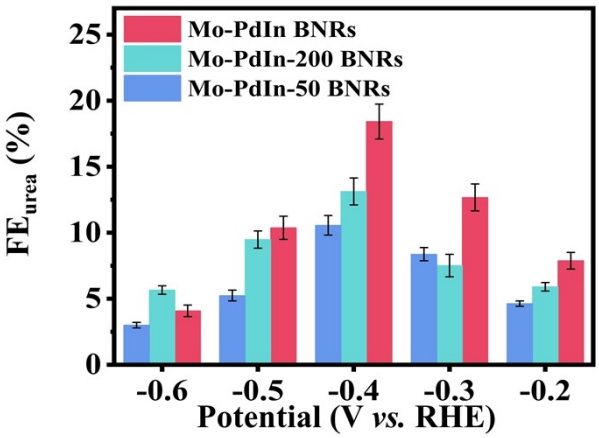

Fig. S17 The FEs of urea with varying contents of Mo-PdIn BNRs at different applied potentials. The atomic ratios of Pd/In in the typical Mo-PdIn BNRs, Mo-PdIn-200 BNRs and Mo-PdIn-50 BNRs are determined to be 6.2/1, 2.3/1 and 7.7/1, respectively.

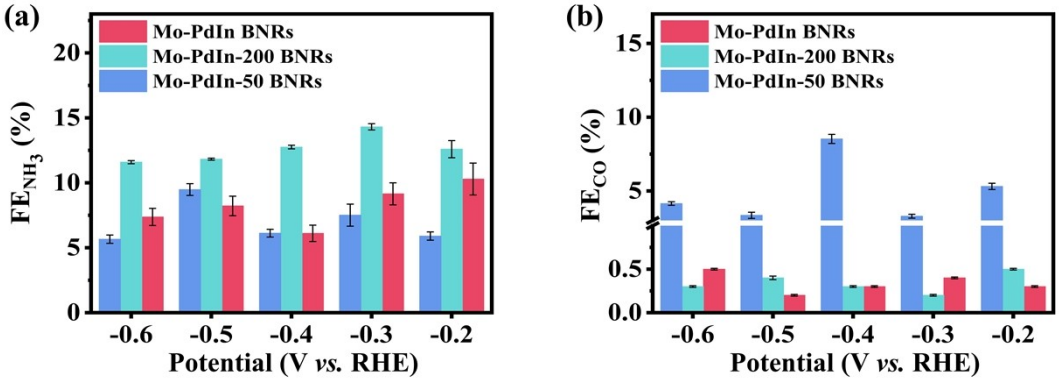

Fig. S18 FEs of (a) NH_3 and (b) CO with varying contents of Mo-PdIn BNRs at different applied potentials.

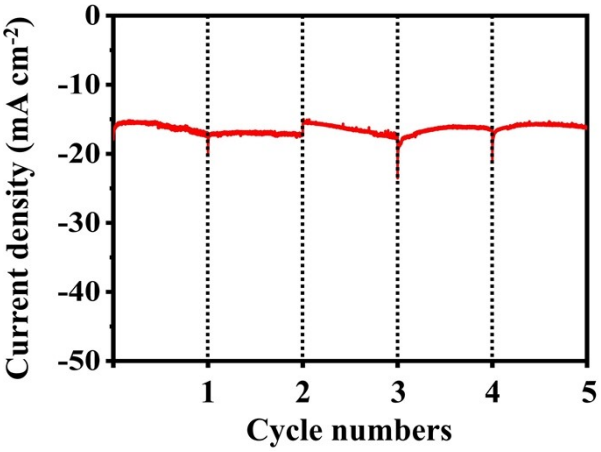

Fig. S19 Chronoamperometric curve of the Mo-PdIn BNRs at -0.4 V *vs.* RHE for 5 cycles (2 h for each cycle).

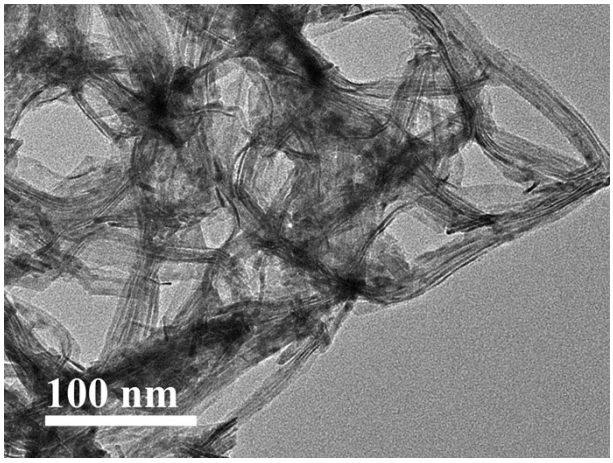

Fig. S20 TEM image of the Mo-PdIn BNRs after cycle testing.

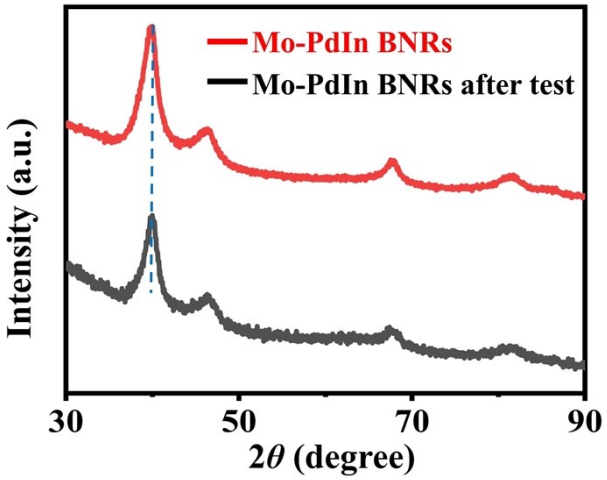

Fig. S21 XRD patterns of Mo-PdIn BNRs before and after cycle testing.

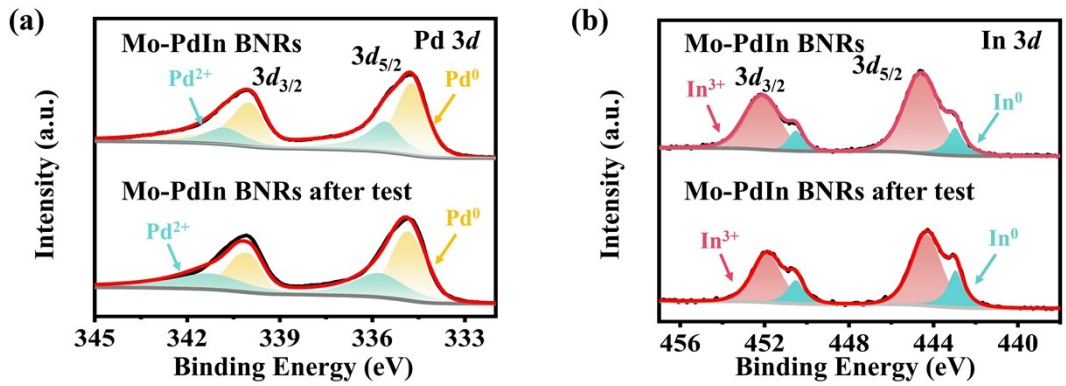

Fig. S22 (a) Pd 3d XPS spectra and (b) In 3d XPS spectra of Mo-PdIn BNRs before and after cycle testing.

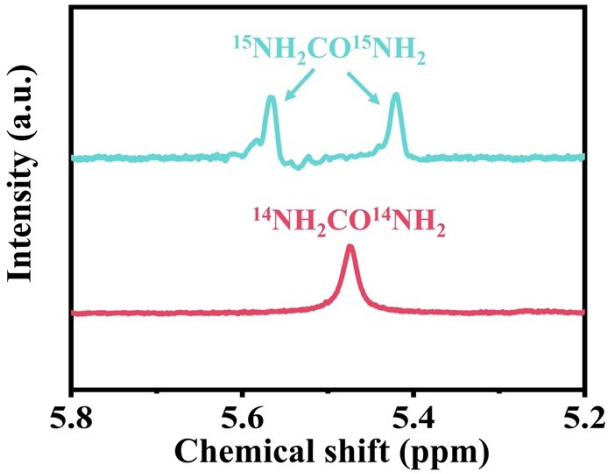

Fig. S23 ^{1}H NMR spectra of urea produced using $^{14}NO_3^-/CO_2$ and $^{15}NO_3^-/CO_2$ as feedstocks respectively.

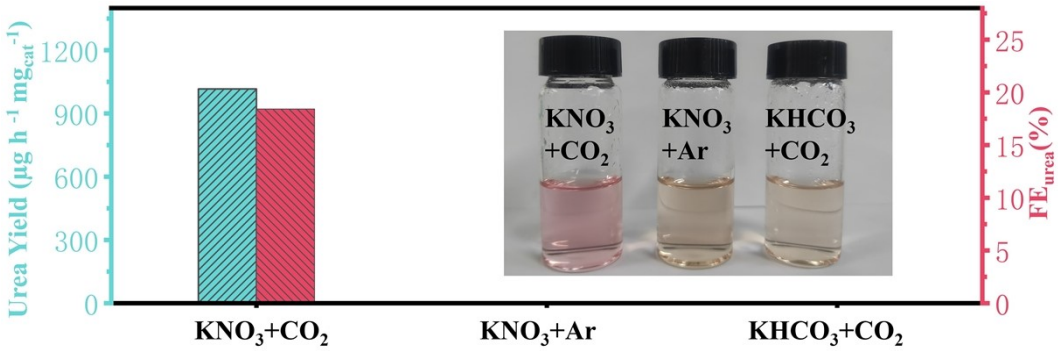

Fig. S24 Comparison of urea yield and FE under different reaction conditions and corresponding color development results.

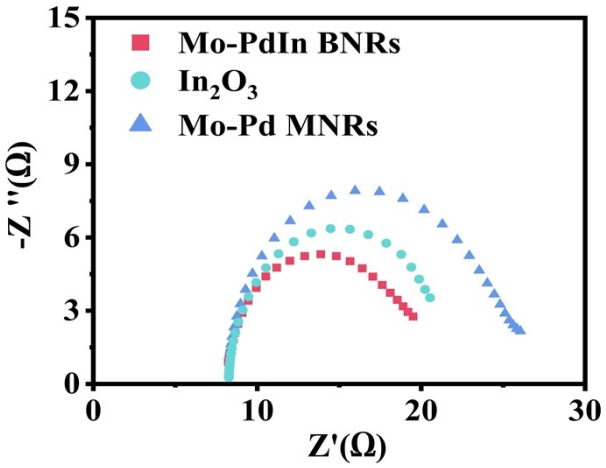

Fig. S25 EIS spectra of Mo-PdIn BNRs, In_2O_3 and Mo-Pd MNRs catalysts at -0.4 V *vs.* RHE in a frequency ranging from 100 kHz to 0.1 Hz.

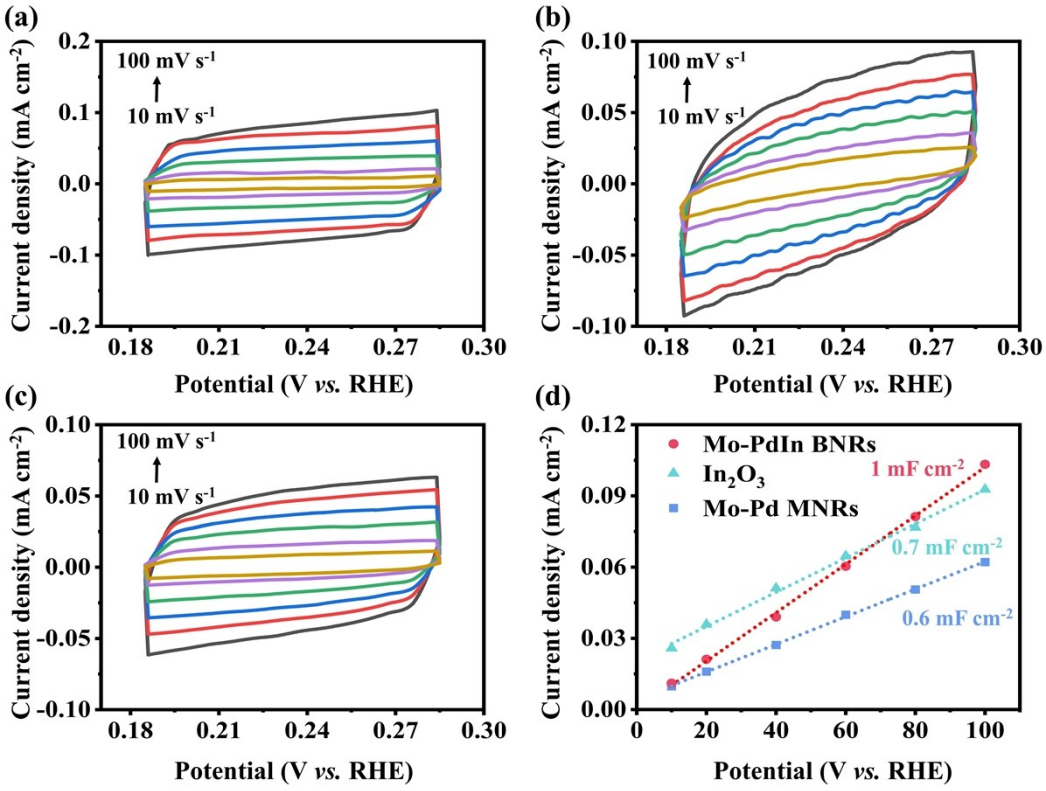

Fig. S26 CV curves of catalysts under various scan rates from 10 to 120 mV s^{-1}: (a) Mo-PdIn BNRs, (b) In_2O_3 and (c) Mo-Pd MNRs. (d) The calculated C_{dl} values.

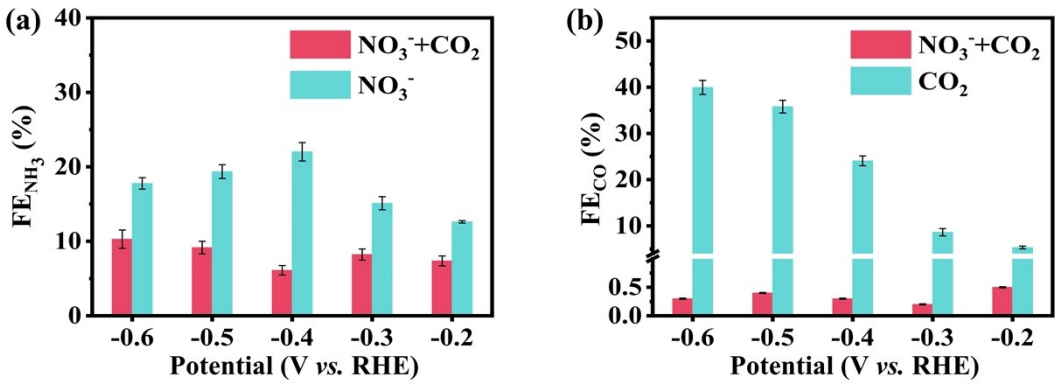

Fig. S27 (a) NH_3 FEs of Mo-PdIn BNRs for NO_3^-RRand C-N coupling reaction. (b) CO FEs of Mo-PdIn BNRs for CO_2RR and C-N coupling reaction.

Table S1 The atomic ratios of various samples determined by ICP-OES.

Samples	Atomic ratio
Mo-PdIn BNRs	Pd/In/Mo = 82.84/13.33/3.83
PdIn BNRs	Pd/In = 85.64/14.36
Mo-Pd MNRs	Pd/Mo = 95.40/4.60

Table S2. Comparison of electrocatalytic performance of Mo-PdIn BNRs toward urea synthesis with previously reported catalysts.

Catalysts	Reactant	Yeild rate ($\mu g\ h^{-1} mg_{cat}^{-1}$)	FE_{urea} (%)	Potential (V *vs.* REH)	Ref.
Mo-PdIn BNRs	**CO_2 + 0.1 M KNO_3**	**1016.49**	**18.42**	**-0.4 V**	**this work**
$BiFeO_3/BiVO_4$	N_2 + 0.1 M $KHCO_3$	297.3	17.18	-0.4 V	3
CuPc NTs	N_2 + 0.1 M $KHCO_3$	143.47	12.99	-0.6 V	4
$PdCu/TiO_2–V_o–400$	N_2 + 0.1 M $KHCO_3$	201.8	8.92	-0.4 V	5
Fe(a)@C-Fe_3O_4/CNTs	CO_2 + 0.1 M KNO_3	1341.3	16.50	-0.65 V	6
Fe^{II}-Fe^{III}OOH@$BiVO_4$	CO_2 + 0.1 M KNO_3	828.83	11.50	-0.8 V	7
V_o-CeO_2-750	CO_2 + 0.1 M $KHCO_3$ + 0.05 M KNO_3	943.6	4.00	-1.6 V	8
Vo-InOOH	CO_2 + 0.1 M KNO_3	592.5	51.00	-0.5 V	9

References

1. M. Sun, G. Wu, J. Jiang, Y. Yang, A. Du, L. Dai, X. Mao and Q. Qin, *Angew. Chem. Int. Ed.*, 2023, **62**, e202301957.
2. P. Zhan, J. Zhuang, S. Yang, X. Li, X. Chen, T. Wen, L. Lu, P. Qin, B. Han, *Angew. Chem. Int. Ed*., 2024, **63**, 202409019.
3. M. Yuan, J. Chen, Y. Bai, Z. Liu, J. Zhang, T. Zhao, Q. Shi, S. Li, X. Wang and G. Zhang, *Chem. Sci.*, 2021, **12**, *6048-605*8.
4. J. Mukherjee, S. Paul, A. Adalder, S. Kapse, R. Thapa, S. Mandal, B. Ghorai, S. Sarkar and U. K. Ghorai, *Adv. Funct. Mater.*, 2022, **32**, 2200882.
5. C. Chen, X. Zhu, X. Wen, Y. Zhou, L. Zhou, H. Li, L. Tao, Q. Li, S. Du, T. Liu, D. Yan, C. Xie, Y. Zou, Y. Wang, R. Chen, J. Huo, Y. Li, J. Cheng, H. Su, X. Zhao, W. Cheng, Q. Liu, H. Lin, J. Luo, J. Chen, M. Dong, K. Cheng, C. Li and S. Wang, *Nat. Chem.*, 2020, **12**, 717-724.
6. J. Geng, S. Ji, M. Jin, C. Zhang, M. Xu, G. Wang, C. Liang and H. Zhang, *Angew. Chem. Int. Ed.*, 2023, **62**, e202210958.
7. H. Yin, Z. Sun, Q. Zhao, L. Yang, T. Lu and Z. Zhang, *J. Energy Chem.*, 2023, **84**, 385-393.
8. X. Wei, X. Wen, Y. Liu, C. Chen, C. Xie, D. Wang, M. Qiu, N. He, P. Zhou, W. Chen, J. Cheng, H. Lin, J. Jia, X. Z. Fu and S. Wang, *J. Am. Chem. Soc.*, 2022, **144**, 11530-11535.
9. C. Lv, C. Lee, L. Zhong, H. Liu, J. Liu, L. Yang, C. Yan, W. Yu, H. H. Hng, Z. Qi, L. Song, S. Li, K. P. Loh, Q. Yan and G. Yu, *ACS Nano*, 2022, **16**, 8213-8222.